ISSN Application No. 21651

Journal of Mechanics and Thermodynamics

Volume No. 13
Issue No. 2
May - August 2025

ENRICHED PUBLICATIONS PVT.LTD

JE - 18,Gupta Colony, Khirki Extn,
Malviya Nagar, New Delhi - 110017.
E- Mail: info@enrichedpublication.com
Phone :- +91-8877340707

ISSN Application No. 21651

Journal of Mechanics and Thermodynamics

Aims and Scope

Journal of Mechanics and Thermodynamics publishes theoretical and practice oriented papers, dealing with problems of modern technology (power and process engineering, structural and machine design, production engineering mechanism and materials, etc.), Materials and Design Engineering, Vibration and Control, Thermal Engineering and Fluids Engineering.

ISSN Application No. 21651

Journal of Mechanics and Thermodynamics

ISSN Application No. 21651

Journal of Mechanics and Thermodynamics

(Volume No. 13, Issue No. 2, May - August 2025)

Contents

ISSN Application No. 21651

Experimental Studies on Di Diesel Engine Using Pre Heated Cotton Seed Oil Ethyl Ether as Alternative Fuel

K.Kusuma1 and Dr. E.L.Nagesh2
1Research Scholar, Department of Mechanical Engineering, JNTUH, Hyderabad,
2Professor, St.Peter's Engineering college,

ABSTRACT

In this investigation, the Cotton Seed Oil Di-Ethyl Ether (CSODEE) was prepared by transesterification using cotton seed oil, Di-Ethyl Ether and potassium hydroxide (KOH) as a catalyst. At different preheated temperatures, the performance and exhaust emissions of a diesel engine fuelled with preheated CSODEE were obtained and compared with neat diesel. Experiments were conducted at different load conditions in a single cylinder four stroke DI diesel engine. CSODEE was preheated to temperatures namely 30, 40, 60, 80, 100ºC before it was fuelled to the engine. From the test the brake thermal efficiency (BTE), brake specific fuel consumption (BSFC), smoke density, CO, HC, NOx emissions were evaluated. The results proved that the preheated CSODEE leads favorable on BTE and CO, HC emissions when it is heated up to 80ºC. At the same time the NOx emission was increased. But at preheated temperature of 100°C, a considerable decrease in the BTE and BSFC were observed due to the vapour locking in the fuel line caused by vapour formation due to higher temperature of CSODEE. On the whole the results shows that CSODEE preheated up to 80ºC can be used as an alternate fuel for diesel fuel without any significant modification in expense of increased NOx emissions.

Keywords : *Cotton seed oil ethyl ether, Diesel engine performance, Exhaust emissions, Pre-heated biodiesel*

1. INTRODUCTION

The idea of using vegetable oil began in the year 1893 itself when diesel engines came into existence. In the year 1911, Rudolf Diesel operated his first engine using straight vegetable oil (peanut oil). The physical and combustion properties of vegetable oils are closer to that of diesel and in this context; vegetable oils can stand as an immediate candidate to substitute for fossil fuels. The greatest advantages of vegetable oils are that they are obtained from seeds of various plants. In view of this, researchers have started showing renewed interest towards vegetable oils because of its advantages as a potential alternate fuel. Vegetable oils are renewable and ecofriendly in nature and at the same time, it can be easily produced in rural areas. Sustainable development of a country depends on the extent that it is managing and generating its own resources. This also helps in conservation of depletion of nonrenewable petro-products. However due to inherent high viscosity and low volatility, vegetable oils would pose problems such as fuel flow and poor atomization and constrain their direct use in engine without any modifications vegetable oils are either edible or non-edible. Some of the edible oils are sunflower oil, palm oil, rice bran oil, and cottonseed oil. The non-edible oils are mahua oil, jatropha oil, rubber seed oil, etc. As rice bran and cottonseed oil (CSO) are not very much in use for cooking purpose, these can be used as substitute for diesel in CI engines. Cottonseed oil has several properties closer to that of diesel but certain properties such as high viscosity and low volatility pose problem when used as an alternate fuel for C.I engines.

The potential of using vegetable oil for diesel engines was studied by Recep Altin et al. [1], Yoshomoto .y et al. [2] and Kensuke Nishi et al.[3]. The engine performance was very much similar to that for diesel with little power loss and slight increase in the emission level. Karaosmanoglu.F et al[4] studied long-term utilization of vegetable oil and no significant increase or loss in power was noticed. Nwafor O.M.I et al. [5] carried out combustion studies on both diesel fuel and vegetable oil fuel with standard and advanced injection timings. Advanced injection timing compensates the effects of the longer delay period and slower burning rate that is exhibited by vegetable oils. The problems related to low volatility and high viscosities are offset by subjecting the oil into the process of transesterification, and the high viscosity can be reduced. Methyl and ethyl esters of vegetable oil (called as bio-diesel) have the physical and chemical properties closer to that of diesel. The performance and emission characteristics of the diesel engine using methyl ester are comparable with that of diesel as per Dilip Kumar Bora et al. [6]. Babu A.k et al. [7] also has reported problems related to high viscosity. Blending vegetable oil with diesel decreases the viscosity and improves the volatility. This improved properties results in better mixture formation and spray penetration. A number of investigators tried the vegetable oils in varying proportions with diesel. Results obtained from experiments shows that vegetable oil and diesel blends showed improvement in engine performance [8, 9]. Pre heating the vegetable oil reduces the viscosity and improves combustion characteristics (Pramanik. K [10]). This paper examines the use of preheated cottonseed oil diesel blends on the performance of a single cylinder diesel engine. Preheating the vegetable oil decreases the viscosity and improves the atomization and mixing process, which results in better combustion.

2. PRODUCTION OF COTTONSEED OIL DI-ETHYL ETHER

Cotton seed oil was converted into biodiesel through the alkaline transesterification reaction for which potassium hydroxide was used as catalyst with methanol. Two percent of the potassium hydroxide catalyst was dissolved in DEE (30% by weight) and the mixture was added to the cotton seed oil. Then the prepared mixture was stirred at 60^{o}c for 30 minutes. There after the reactant material was poured into transparent vessel and allowed for cooling at room temperature for 7-8 hours. It was allowed to settle for separation of glycerol as bottom layer. The upper layer of biodiesel was kept into another vessel for washing with equal amount of water. The biodiesel was heated up to 110^{o}c for 15 minutes to remove excess water. Then biodiesel was cooled down to room temperature before use, presenting a 94% yield. Transesterification, which is also called alcoholics, is a process of substitution of the radical of an ester by the radical of one alcohol, like hydrolysis. The biodiesel was produced from cotton seed oil in our lab. Density of the fuel was found using density bottle, kinematic viscosity of the oil was determined with the help of Redwood Viscometer and flash point was obtained from electrically heated Pesky-Martens apparatus as per the standard test procedure. The gross calorific value of the cotton seed oil, cotton seed ethyl ether and diesel were determined with the help of Bomb calorimeter.

3. EXPERIMENTAL SETUP AND TEST PROCEDURE

The experiments were conducted on a single cylinder four stroke DI diesel engine as shown in Fig 1. The engine specifications are described in Table 1. The test set up consists of various measuring instruments to measure various parameters like engine torque, air flow rate, fuel consumption, exhaust emissions, temperatures of air and fuel. Experiments were conducted with neat diesel fuel and preheated CSODEE at five different temperatures of 30ºC, 40ºC, 60ºC, 80ºC, 100ºC.

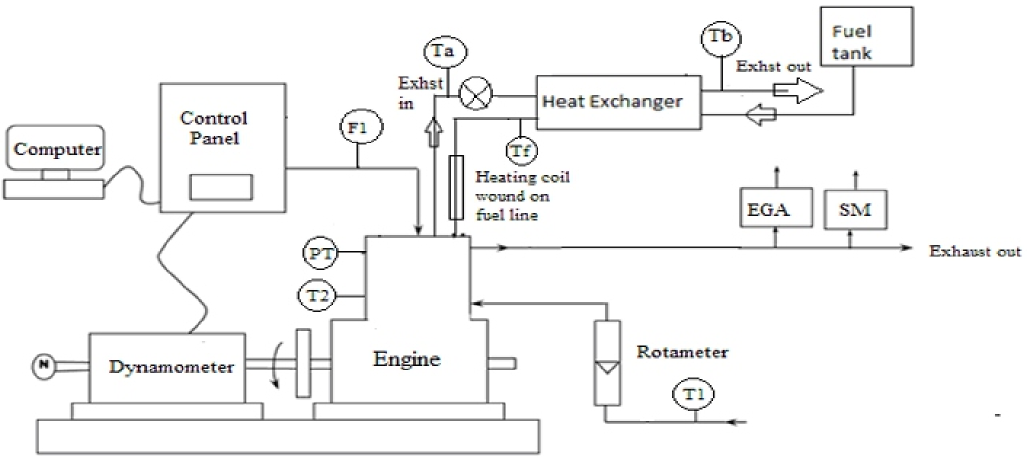

Fig 1: Schematic diagram of the experimental test rig

4

T1- Inlet engine water temperature PT - Pressure transducer N - RPM Decoder

T2 - Outlet engine jacket water temperature Ta, Tb - In and out temperature of exhaust gas in H.E

Tf - Fuel temperature at outlet of H.E F1- Fuel Flow (Differential Pressure unit) EGA - Exhaust Gas Analyzer (5 gas) SM – Smoke Meter

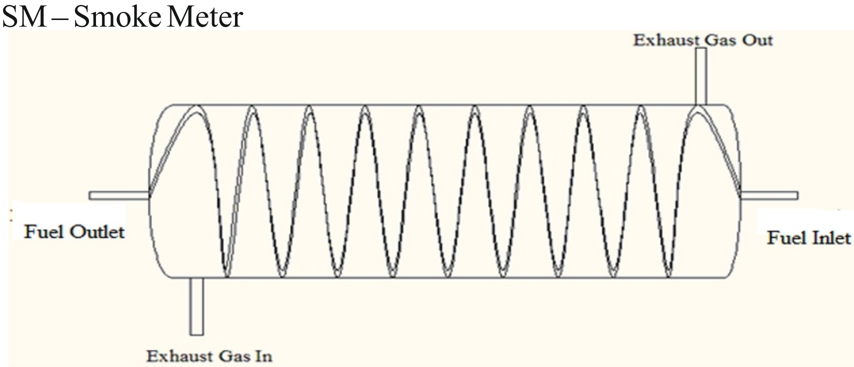

Fig 2: Heat Exchanger

Table.1 Test Engine Specification

Engine	Four-stroke, single cylinder, constant speed, water cooled CI Engine
Make	Kirloskar
Model & BHP	TV1 & 5.2kW@ 1500 RPM
Compression Ratio	17.5:1
Dynamometer Type	Eddy Current, with loading unit
Load Measurement	Strain Gauge Load cell
Interfacing	ADC card- PCI 1050

The engine was connected to an eddy current dynamometer and the engine was running at a constant speed of 1500rpm. Experiments were conducted at the engine speed of 1500 rpm and at different engine loads. Initially the experiments were carried out for the diesel fuel for different loads. The fuel consumption, brake power, brake specific fuel consumption, brake thermal efficiency and exhaust gas temperature were measured. The NOX , CO and HC emission were measured with non-dispersive infra red analyzers. The smoke density is measured by smoke meter. The gas analyzers were calibrated with standard gases and zero gas before each test. Same procedures were repeated for CSODEE at different temperatures namely 30,40,60,80, and100ºC. The physical properties of neat diesel fuel of CSODEE are shown in Table 2,

Table: 2 The properties of diesel fuel and COSDEE

Property	Cotton seed oil	Cotton seed oil Di-Ethyl Ether (CSODEE)	Diesel fuel
Density(g/ml)	0.96	0.926	0.830
Kinematic viscosity, cS at 38^{o}C	226.82	8.58	5.80
Gross calorific value(MJkg^{-1})	36.20	40.16	46.22
Flash point(^{o}C)	317	157	47
Acid value(mgKOH/g)	1.642	1.018	0.00
Free fatty acid content (%)	2.8	1.96	0.00

Table: 3 The Properties of CSODEE at different Temperatures

Temperature of CSODEE(^{o}C)	30	40	60	80	100
Specific gravity	0.872	0.898	0.876	0.867	0.885
Kinematic viscosity(cSt)	7.98	7.85	5.9	4.8	1.9

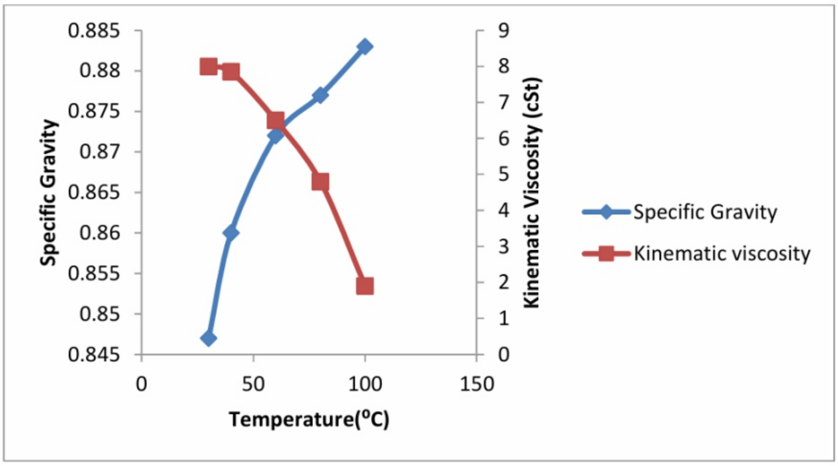

Fig 2: Effect of preheating on the Kinematic viscosity and specific gravity of CSODEE

3.1 Engine Performance and exhaust emissions

The changes of brake specific fuel consumption (BSFC) with brake power for different CSODEE are presented in Fig 3. The BSFC of all CSODEE is higher than that of diesel for all loads. For all CSODEE tested, BSFC is found to decrease with increase in the load. This is due to more blended fuel which is used to produce same power as compared to diesel. The BSFC increased from 556 g/kWhr to 665g/kWhr for diesel and CSODEE 100 respectively at full load. This is due to the effect of higher viscosity and poor mixture formation of CSODEE. But the BSFC is decreased due to increasing the preheating temperature of CSODEE. This is due to the reduced viscosity and improved spray characteristics of CSODEE.

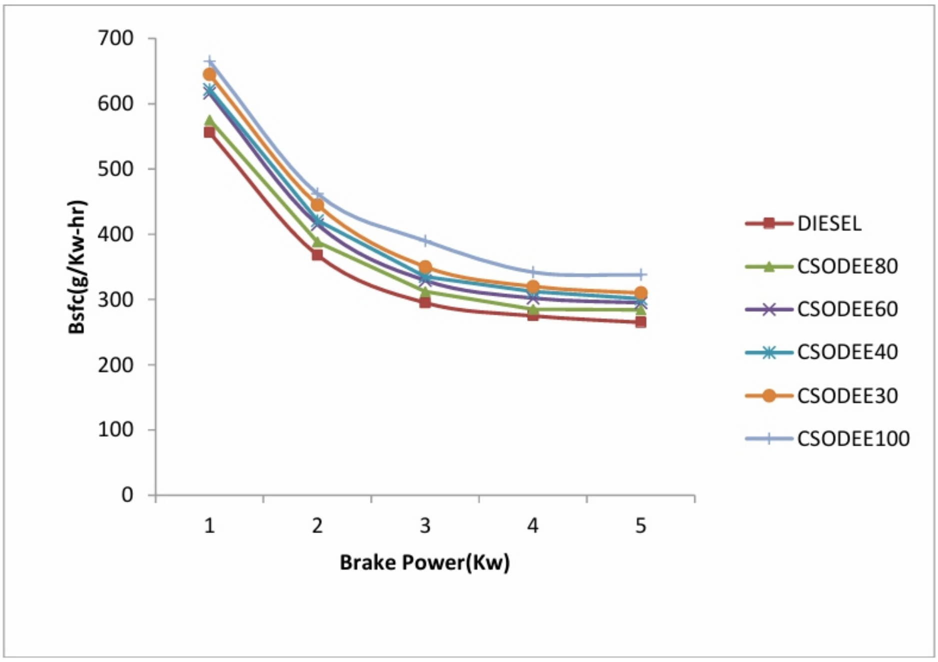

Fig 3: Brake specific fuel consumption

The variation in the brake thermal efficiency (BTE) of the engine fuelled with CSODEE preheated to30ºC, 40ºC, 60ºC, 80ºC and 100ºC which are indicated by CSODEE30, CSODEE40, CSODEE60, CSODEE80, CSODEE100, Respectively, with reference to diesel fuel are shown in Fig 4. The increase in BTE with CSODEE operations can also be attributed to the good combustion characteristics of bio-diesel owing to their decreased viscosity and improving volatility by means of preheating process. It is seen that the BTE of CSODEE increased by the preheated temperature 30ºC, 40ºC, 60ºC, and 80ºC , But for 100ºC the BTE decreases due to vapour locking in the fuel line and hence more fuel consumption is obtained for the same power compared to other mode of operation. The BTE with the CSODEE100 is 5% and 13% lower than that of CSODEE 80 and diesel fuel respectively.

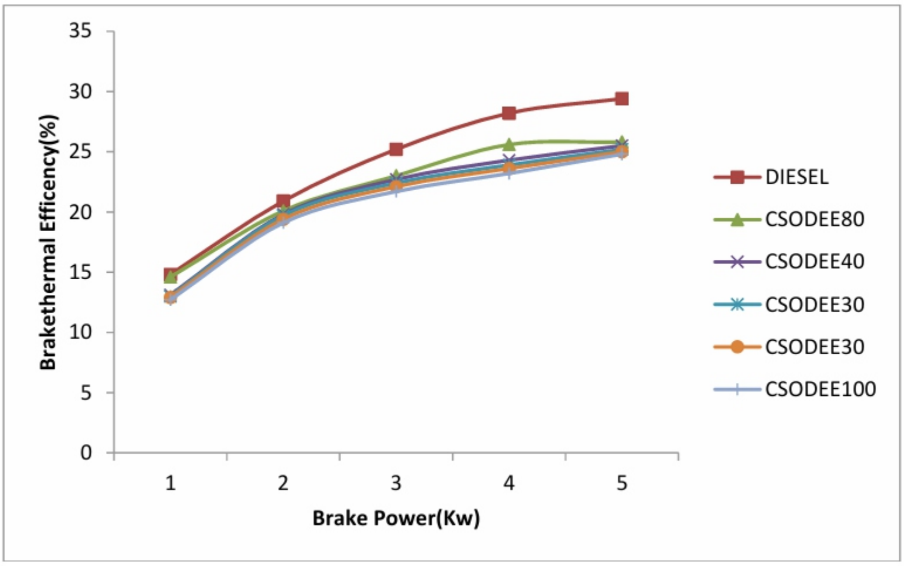

Fig 4: Brake thermal efficiency

The CO emissions are shown in Fig 5. As seen in the figure, the emissions increase with increase of engine load, due to rich fuel air mixture. Compared with the diesel fuel, the CO emissions of CSODEE are lower, because of the higher oxygen content of biodiesel, which could improve the combustion process. Additionally, the heating process decreases the viscosity of biodiesel and improves the oxidation of biodiesel in the cylinder. Therefore, the CO emissions' arising from incomplete combustion is decreased by applying preheating of the fuel. For CSODEE100, the CO emission is higher than that of CSODEE30, CSODEE40, CSODEE60 and CSODEE80, This is due to uneven fuel spray in the combustion chamber, because of vapour locking in the pump and pipe line, CO emissions obtained with CSODEE80 were 13% lower than that of diesel operations at full load.

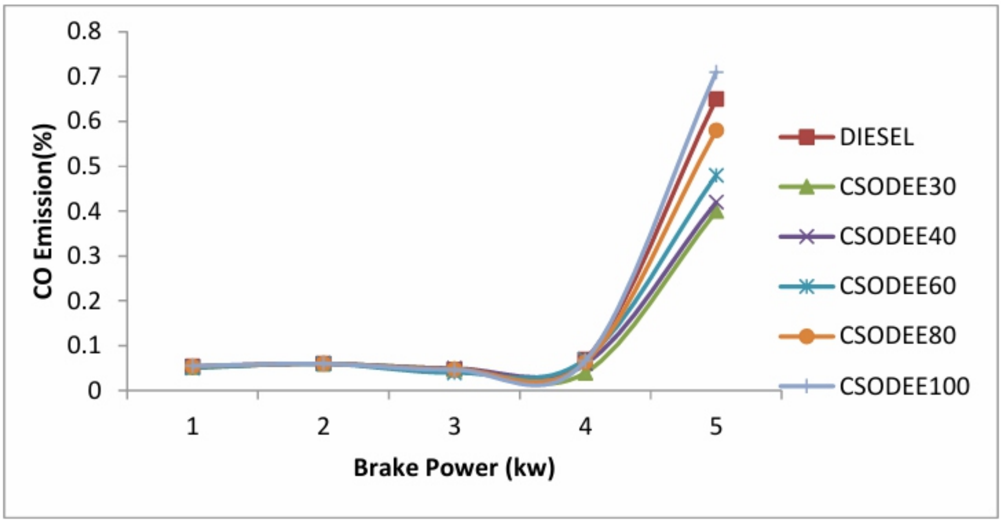

Fig 5: CO Emission Vs Brake Power

Fig 6 shows the variation of HC emissions, similar to the CO emissions, with an increase in the engine load, the HC emissions also decrease. Compared with diesel fuel, CSODEE give lower HC emissions. The HC emissions of CSODEE80 decrease 5.4 % at the maximum load of the engine in comparison with diesel fuel. The higher oxygen content of CSODEE leads to better combustion, resulting in lower HC, However, the HC emissions of CSODEE100 are higher than of other CSODEE. This is due to incomplete combustion occurring at uneven spray characteristics.

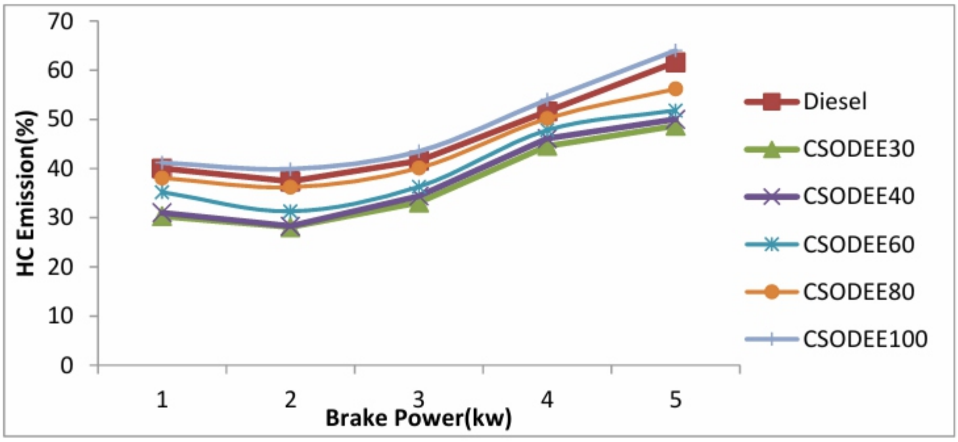

Fig 6: HC Emissions Vs Brake power

Fig7 shows the variation of the NOX emissions of the test engine for CSODEE with reference to diesel fuel. It is seen that the CSODEE operations usually yield higher NOX emissions at all loads compared to diesel fuel operations. The increase in NOX emissions with CSODEE may be attributed to various reasons, such as improved fuel spray characteristics, better combustion of biodiesel due to its high oxygen content and high temperatures in the cylinder as a result of preheating. The maximum increase in NOX emissions were obtained in CSODEE80. The NOX emissions with CSODEE80 increase as compared to diesel fuel at full load.

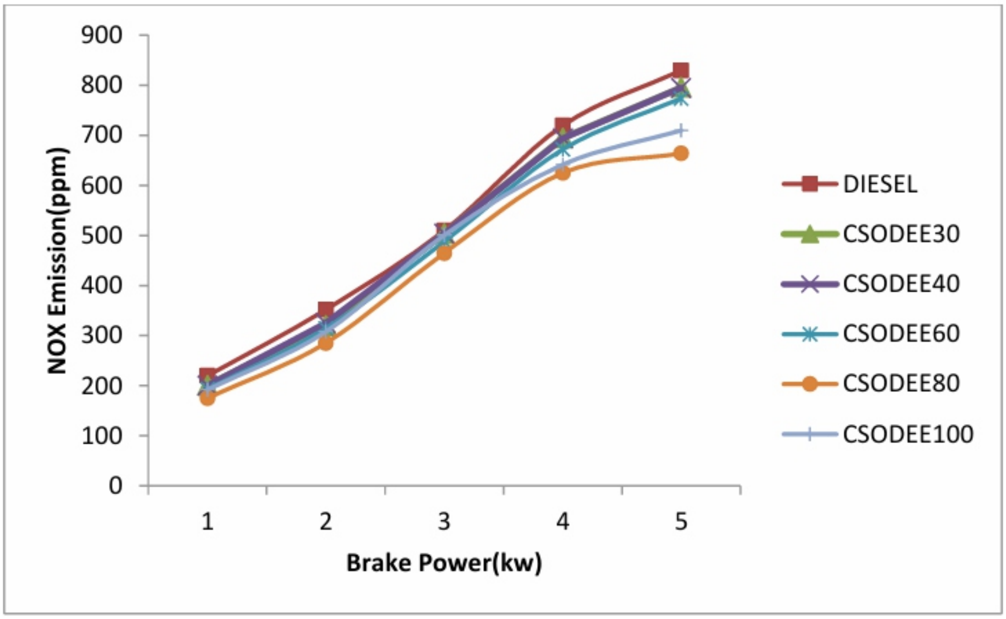

Fig 7: NOx Emission Vs Brake Power

The variation of smoke density for different CSODEE is shown in Fig . The Smoke density of CSODEE is lower than that of the diesel oil. The viscosity of preheated CSODEE is comparatively lower than neat diesel. Due to this, the spray pattern and fuel penetration are improved. But for CSODEE100 the smoke density is slightly higher that of diesel and other CSODEE. This is due to uneven fuel spray pattern in the combustion chamber, because of vapour locking in the pump and pipe line. The smoke density is decreased from 89HSU to 73 HSU for diesel and CSODEE80 respectively at full load.

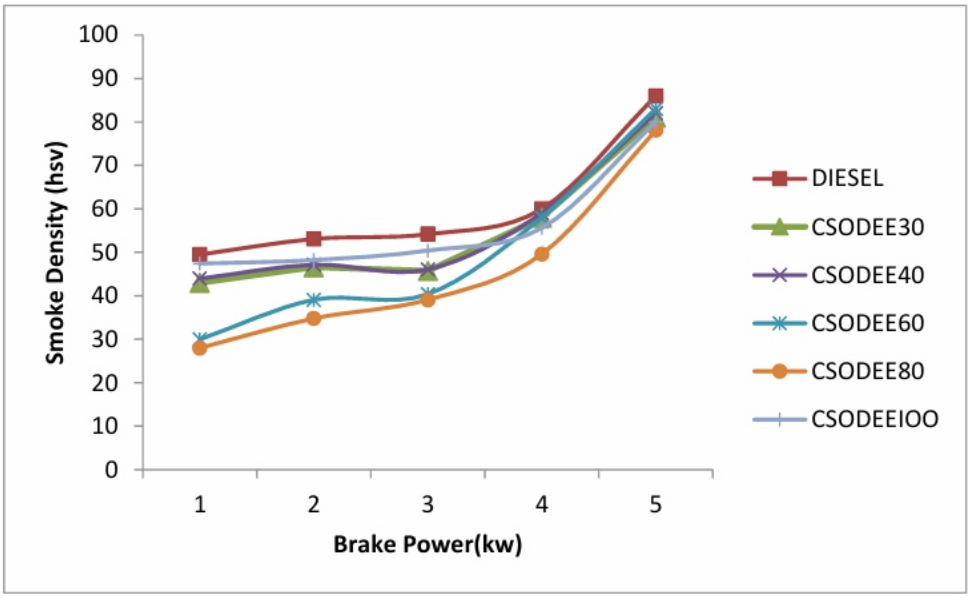

Fig. 8: Smoke density Vs Brake power

CONCLUSIONS

Cottonseed oil Di-ethyl ether (CSODEE) was produced by means of transesterification process using cottonseed oil, which can be described as a renewable energy source. The viscosity of CSODEE was reduced by preheating it before supplied to the test engine. After the fuel properties of CSODEE has been determined, various performance parameters and exhaust emissions of the engine fuelled with CSODEE preheated at different temperatures were investigated and compared with the diesel fuel. The experimental conclusions of this investigation can be summarized as follows:

Preheating of CSODEE makes significant decrease in its kinetic viscosity and a small decrease in specific gravity. It is almost nearer to the values of diesel fuel.

The Brake specific Fuel Consumption (BSFC) increased from 269g/kWhr to 345 g/kWhr for diesel and CSODEE100 respectively at full load.

The Brake Thermal Efficiency (BTE) with the CSODEE100 is 5% and 13% lower than that of CSODEE80 and diesel fuel.

The use of preheated CSODEE produced a considerable decrease in CO emissions. CO emissions obtained with CSODEE80 operations were 34% lower than that of diesel fuel operations.

Compared with diesel fuel, CSODEE gives lower HC emissions, The HC emissions of CSODEE 80 decreases by 16% at maximum load of engine in Comparision with the diesel fuel.

NOX emissions are increased due to higher combustion temperatures caused by preheating and oxygen content of CSODEE. The maximum increase in NOX emissions were obtained in case of CSODEE80. The NOX emissions with CSODEE80 increases approximately 11% as compared to diesel fuel at full load.

The smoke density decreased from 89 HSU to 73 HSU for diesel and CSODEE80 respectively at full load.

In general the performance and emission level of preheated ethyl ether of cottonseed oil are improved. But the NOX emissions are increased due to high combustion temperature and oxygen content in CSODEE.

REFERENCES

[1] Recep Altin, Selim Cetinkaya and Huseyin Sardar Yucesu, et. al "The potential of using vegetable oil fuels as fuel for diesel engines", International Journal of Energy conversion and management Vol. 42, 2001, 529-538.

[2] Y. Yoshimoto, M. Onodera and H. Tamaki, "Performance and emission characteristics of diesel

engines fueled by vegetable oils", SAE Technical Paper Series, Paper No. 2001-01-1807/4227.

[3] Kensuke Nishi, Koji Korematsu and Junya Tanaka, "Potential of rape seed oil as a diesel engine fuel", SAE Technical Paper Series, Paper No.2004-01-1858.

[4] F. Karaosmanoglu, G. Kurt and T. Ozaktas, "Long term C.I engine test of sunflower oil", International journal of Renewable Energy, Vol. 19, 2000, 219-221.

[5] O. M. I. Nwafor and G. Rice, "Performance of rapeseed oil methyl ester in diesel engine", International journal of Renewable Energy, 0960-1481 Vol. 95,199500022-4.

[6] Dilip Kumar Bora, Milton Polly, Vikas Sandhuja and L. M. Das, "Performance evaluation and emission characteristics of a diesel engine using mahua oil methyl ester (MOME)", SAE Technical Paper Series, Paper No. 2004-28-0034.

[7] K. Babu and G. Devaradjane, "Vegetable oil and their derivatives of fuel for C.I engines: An Overview", 01-0767.

[8] O. M. I. Nwafor and G. Rice, "Performance of rapeseed oil blends in a diesel engine", International Journal of Applied Energy, Vol.54, No.4, 1996, 345354.

[9] P. K. Devan and N. V. Mahalakshmi, "Performance, emission and combustion characteristics of poon oil and its diesel blends in a DI diesel engine", Fuel, Vol. 88, 2009, 861-867.

[10] K. Pramanik, "Properties and use of jatropha curcas oil and diesel fuel blends in compression ignition engine", International Journal of Renewable Energy, Vol. 28, 2003, 239-248.

ISSN Application No. 21651

Numerical Investigation of Transient Solidification Behavior of Cast with and without Feeding Aids

Lokesh Baviskar[1] and Dr. R. S. Maurya[2]

1P.G student, Sardar Patel College of Engineering, Mumbai, India.

2Associate Professor, Sardar Patel College of Engineering, Mumbai, India.

ABSTRACT

Sand casting is one of the oldest manufacturing process applicable for mass production of varieties of product. Through the pouring cup molten metal is poured into mould cavity which made in same as size of product. The molten metal is then allowed to cool and solidify. There is occurrence of liquid shrinkage and solid shrinkage while solidification of casting take place. The riser which is reservoir of molten metal is placed to compensate this shrinkage of molten metal. To serve this purpose the solidification time of riser should be greater than solidification time of casting. The riser sleeve and hot toping are the most widely used feeding aids which use to elongate solidification time of riser. The objective of the present work is to assess the transient behavior of solidification of cast with and without sleeve (exothermic) and hot-toppings (exothermic). The investigation is executed using commercial software ANSYS Fluent.

Keywords: *Sand casting, casting solidification, exothermic sleeve, hottoping, ANSYS Fluent, heat generation rate, hottoping thickness*

1. INTRODUCTION

Sand casting is one of the oldest manufacturing process applicable for mass production of varieties of product. Through the pouring cup molten metal is poured into mould cavity which made in same as size of product. The molten metal is then allowed to cool and solidify. There is occurrence of liquid shrinkage and solid shrinkage while solidification of casting take place. To compensate this shrinkage, the reservoir of molten metal is placed above casting which is called as riser. So in simple word the purpose of riser is to supply molten metal to casting when solidification of casting take place. But this purpose can only be serve when casting solidify before riser gets solidify. This means that solidification time of riser should be greater than solidification time of casting. For that casting gating system design is carried out in such manner that will it ensure that riser gets solidify at last. But practically when casting is poured it is just possibility that riser gets solidify at last. So another remedy is to elongate solidification time of riser by used of feeding aids. The riser sleeve and hot toping are the most widely used feeding aids. The purpose of these feeding aids is to improve riser efficiency by controlling heat loss from the riser or by providing an additional heat source to the metal in the riser. The riser sleeve can be either insulating or exothermic or with a combination of both properties. The riser sleeves are made up of thermite materials, initiator and insulating materials. Various suppliers produce these sleeves in different compositions, different size and shapes. As soon as molten metal, contacts with sleeve or hottoping the exothermic reaction take place with the liberation of heat until exothermic material burns. The mushy zone is a transition region between metal which is solidified and which is in liquid state.

Wlodwar et al. [1] conducted various experiment in which involve the surrounding spherical casting with exothermic material lining and corresponding increase in thickness of sleeve lining. He obtain different solidification time for different thickness of lining. In another experimentation Wlodwar et al. found that a sleeve thickness 0.15 times the diameter of the cylinder result in flat shrinkage cavity compare to normally occurring conical shape. All this Wlodwar et al. finding are applicable for particular configuration of geometry and materials, so these finding cannot be generalized. The Foseco [2] recommended sleeve thickness of 0.2 times riser diameter for some categories of sleeve produced by Foseco. Despite the extent of sleeve use, a survey of foundries found that there is lack of consensus on the use of the riser sleeve. Sleeve suppliers use different raw materials of unknown and proprietary compositions and properties in their manufacturing process. As a result application of riser sleeves in foundries is largely based on trusting suppliers, guesswork and trial and error testing [3]. There is no generalized criteria of sleeve thickness for particular casting.

This all leads to use computer casting simulation software for evaluation of effect of riser sleeve and optimization of riser size so that to minimize the defects occurring in the casting. The accurate thermo physical properties of riser sleeve and casting material are required as input data for simulations. These thermophysical properties are either provided by a limited number of suppliers for their products as black box database (hidden from software user) in some commercial casting software like MAGMASOFT or not available. More recently Midea et al. [4] has done investigation on thermophysical data for casting process simulation and have been published temperature dependent curves for density, specific heat and thermal conductivity of several sleeves. But these curves no numerical values are shown on axes so only reader only gets graphical trend of variation of thermal properties with temperature. It was found that thermal conductivity about 4 times more influential than the heat capacity of the sleeve. Iganszak et al. [5] instead of developing temperature dependent data, utilize inverse modelling technique to determined average exothermic sleeve material thermophysical property data. The temperature data in sand mold and steel were obtain by conducting experiments. A computer program was then used to conduct simulations of the castings where all thermophysical properties were iteratively modified until the error between simulation results and measured data is minimized.

R. Hardin et al. [6] studied the effect of sleeve type on casting yield using Magmasoft software. He found that longest solidification time obtain with insulating sleeve while considering 10% safety margin. R. Hardin et al. [7] conducted investigation on determination of thermophysical properties of riser sleeve and casting material using inverse modeling technique of 11 commercial available sleeve. There is no much variation in density and specific heat with respect to temperature. So we can take average and predetermine values of these properties. Iteratively the data for thermal conductivity is developed. MEF is found to be sensitive to superheat and independent of size. Choudari et al. [8] has perform transient thermal analysis using ANSYS software for optimization and analysis of riser in sand casting. Application of sleeve help in reducing riser dimension from 60 mm to 50 mm and thereby increasing the casting yield. Wiwik et al. [9] has done investigation on feeding efficiency between a dome shape and cylinder shape exothermic-insulating sleeve. The casting yield is increased by 90% by dome sleeve greater than cylinder sleeve which have 88% and sand riser which only 19%. A die casting with anti-gravity filling process was numerically investigated using fluent by Yuwen et al. [10] in which Volume of Fluid model used capture filling process. He simulate liquid metal free surface and temperature distribution at various time step. The change in free surface shows that liquid metal is volatile and turbulent at early stage of filling process, when liquid metal contact with mould wall.

Overall sleeve performance depends on the quality and quantity of thermite material present in sleeve. The exothermic heat generation in sleeve and burn time of thermite are the parameter which play important role in determination of riser sleeve effectiveness. Very few literature is observed on the effect of riser sleeve shape on casting performance. There is little work available for investigation of geometrical parameters like thickness of riser sleeve and hottoping on solidification behavior.

2. PROBLEM DEFINITION AND METHODOLOGY

Present problem deals with cast solidification where apart from regular elements of casting system, few other elements are also used to enhance its quality and yield. Use of risers and hot-toppings are very common, which help to increase the casting yield, minimize defects and provides better control on overall casting process. To carry out the investigation a rectangular casting block of dimension 50 mm × 50 mm × 20 mm is considered which is sand casted. An arrangement of mould with feeding element and riser is shown in fig.1. Molten metal (material-ASTM WCB A216) is poured into mould cavity at 1600 °C and solidification takes place. The progress of solidification of molten metal is investigated. The objective of the present work is to assess the transient behavior of solidification of cast with and without sleeve (exothermic) and hot-toppings (exothermic). The investigation is executed using commercial software ANSYS Fluent.

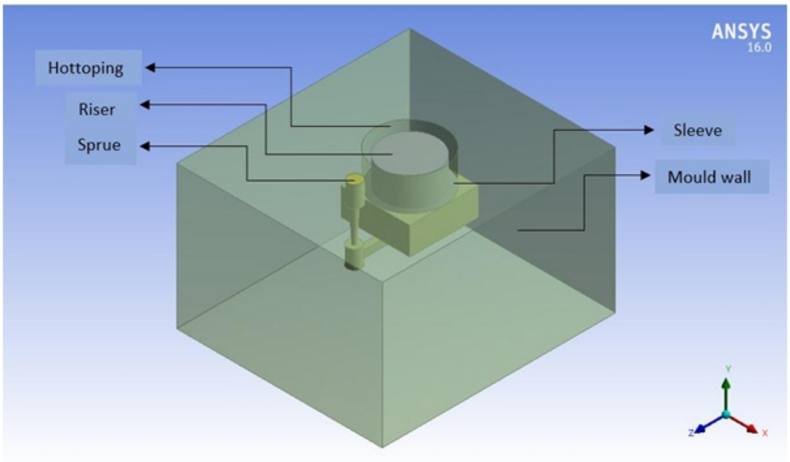

Figure 1: Casting with sand mould

3. THEORETICAL DESIGN OF CASTING SYSTEM

Theoretical design of casting system consist of design of riser, casting gating system and pattern design. The gating system is part of the mould cavity through which the metal is poured to fill the casting impression. Theoretical design of casting is needed to meet following threefold purpose-1) The metal flow rate and direction must be such as to ensure complete filling of the mould before freezing. 2) To avoid entrapment of air, metal oxidation, and mould erosion flow should be smooth and uniform with minimum turbulence. 3) The technique should promote the ideal temperature distribution within the completely filled mould cavity. So that the pattern of subsequent cooling is favorable to feeding. Purpose of riser is to supply molten metal to take care of liquid shrinkage and solid shrinkage. In casting modulus is defined as ratio of volume of casting to surface of casting. Here Riser is design using modulus method. Nonpressurized gating system design is done with gating ratio 1:4:4. Final summary of theoretical design is as shown in table no. 1

Table 1: Casting system dimension

Design parameter	Dimension
Diameter of riser	0.04 m
Height of riser	0.02m
Bottom CS area of sprue	$1.0112 \times 10^{-5} m^2$
Top CS area of Sprue	$2.0224 \times 10^{-5} m^2$
Taper of sprue	0.5
Area of ingate	$4.0448 \times 10^{-5} m^2$
Area of runner	$4.0448 \times 10^{-5} m^2$

4. MATHEMATICAL MODEL

Solidification simulation of casting involves filling of molten metal inside cavity and subsequent solidification of molten metal with respect to time. This process can be described by mass conservation equation, N-S equation, conservation of energy equation, volume of fluid function equation and enthalpy-porosity equation to model solidification process.

- Mass equation : $\frac{\partial u}{\partial x} + \frac{\partial v}{\partial y} + \frac{\partial w}{\partial z} + \frac{\partial p}{\partial t} = 0$ .... (1)

- X-momentum equation

$$\rho\left(\frac{\partial u}{\partial t} + u\frac{\partial u}{\partial x} + v\frac{\partial u}{\partial y} + w\frac{\partial u}{\partial z}\right) = \rho g_x - \frac{\partial p}{\partial x} + \mu\left(\frac{\partial^2 u}{\partial x^2} + \frac{\partial^2 u}{\partial y^2} + \frac{\partial^2 u}{\partial z^2}\right) + s_1 \quad \ldots\ldots (2)$$

Y-momentum equation

$$\rho\left(\frac{\partial u}{\partial t} + u\frac{\partial v}{\partial x} + v\frac{\partial v}{\partial y} + w\frac{\partial v}{\partial z}\right) = \rho g_y - \frac{\partial p}{\partial y} + \mu\left(\frac{\partial^2 v}{\partial x^2} + \frac{\partial^2 v}{\partial y^2} + \frac{\partial^2 v}{\partial z^2}\right) + s_1 \quad \ldots.. (3)$$

Z-momentum equation

$$\rho\left(\frac{\partial u}{\partial t} + u\frac{\partial w}{\partial x} + v\frac{\partial w}{\partial y} + w\frac{\partial w}{\partial z}\right) = \rho g_z - \frac{\partial p}{\partial z} + \mu\left(\frac{\partial^2 w}{\partial x^2} + \frac{\partial^2 w}{\partial y^2} + \frac{\partial^2 w}{\partial z^2}\right) + s_1 \quad \ldots (4)$$

- Energy equation : $\rho c_p \, [\frac{\partial T}{\partial t} + (\vec{V} \cdot \nabla)\ \mathrm{T}\ ] = \mathrm{k}\ \nabla^2 + s_2$ ....(5)

- Volume of fluid : The volume of fluid model can model two or more immiscible fluid phases in terms of volume fraction γ of each of the fluids by solving a single set of mass and momentum equations.

$$\rho = \{\gamma\rho + (1-\gamma)\rho_1\} \quad \ldots\ldots.. (6)$$

$$T = \{\gamma T_1 + (1-\gamma)T_2\} \quad \ldots\ldots.. (7)$$

- Enthalpy-porosity equation : An enthalpy-porosity technique is used for modeling the solidification/melting process. The mushy zone is treated as a "pseudo" porous medium with porosity varying from 0 to 1. In case of fully solidified material in a cell, the porosity becomes zero and thereby the velocity drop to zero. For that purpose additional sink term are added to momentum and energy equation. The momentum sink due to the reduced porosity in the mushy zone takes the following form:

$$s_1 = \frac{(1-\alpha)^2}{(\alpha^3+\epsilon)} A_{mush}\,(\vec{u} - \vec{u}_p) \quad \ldots\ldots. (8)$$

where α is the liquid volume fraction, $\in$ is a small number (0.001) to prevent division by zero, Amush is the mushy zone constant, and $\vec{u}_p$ is the solid velocity due to the pulling of solidified material out of the domain.

Sinks are added to all of the energy equations in the mushy and solidified zones to account for the presence of solid matter.

$$s_2 = \frac{(1-\alpha)^2}{(\alpha^3+\in)} A_{mush}\, \emptyset \qquad \text{......} \ (9)$$

Where $\emptyset$ represents the turbulence quantity being solved ($k, \in, \omega$ etc.)

5. NUMERICAL IMPLEMENTATION AND SOLUTION STRATEGY

Numerical implementation involves preprocessing, solver setting and solver execution. Computational domain consists of rectangular casting block, cylindrical riser and gating system surrounded by moulding sand. Over that is domain conformal mesh with 3D tetrahedron elements were generated using ANSYS meshing modeler. The simulation is carried out by employing energy, viscous laminar, multiphase volume of fluid and solidification & melting model. The multiphase volume of fluid model was used to filled casting with material ASTM A216 WCB steel. To capture solidification of molten metal solidification & melting model was used. Thermophysical properties of ASTM A216 WCB carbon steel, moulding sand as shown in the following table no. 2 & 3

Table 2: Properties of ASTM WCB A216

Properties of ASTM WCB A216	
Density	7800 Kg/m^3 (at 273K)
	7400 Kg/m^3 (at 1273K)
	6800 Kg/m^3 (at 1923K)
Specific heat	1025 J/kg K
Thermal conductivity	55 W/m K (at 273K)
	140 W/m K (at 1923K)
Latent heat	192000 J/Kg
Solidus Temperature	1350 °C
Liquidus Temperature	1500 °C

Table 3: Properties of sand and exo sleeve & hottoping

Properties of sand	
Density	1495 Kg/m^3
Specific heat	1172.304 J/kgK
Thermal Conductivity	0.519 W/m K
Exo sleeve & hottoping	
Density	422 kg/m^3
Specific heat	450 J/kg-K
Thermal conductivity	0.35 W/mk
Ignition Temperature	600 °C
Exothermic Heat Generation	250 KJ/Kg

In simulation process, pouring temperature is 1600°C ; the sand mold and ambient temperature both set to 27°C ; pouring rate is 0.4953 m/s using the way of antigravity bottom pouring ; acceleration due gravity is 9.8 m 2. Boundary conditions were set as follow:1) Sprue top was set as velocity inlet 2) Riser top was set as pressure outlet3) Sand mould wall was set as wall with convection heat transfer coefficient 20 W 2k.

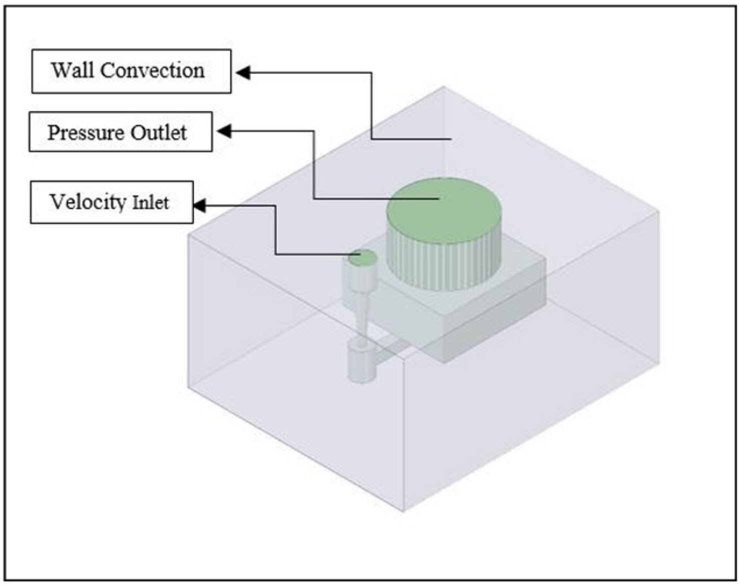

Figure 2 Boundary conditions

For volume of fluid model volume fraction at sprue inlet and riser outlet is set top one and zero respectively. Couple algorithm was used to solve the coupling problem between velocity components and pressure in momentum equations. Momentum,energy were taken as second order upwind scheme runner. So riser is solidifying before casting and it is not serving it purpose of supplying molten metal. This may be due to heat diffusion through top of mould is more as compare to bottom of mould. To get favorable temperature gradient extra sand is added on the top riser and following cases of simulations are investigated with all simulations setting similar to previous simulation- 1) 70 mm sand above riser 2) 50 mm sand above riser 3) 20mm sand above riser

To determine solidification temperature 5 points are taken along vertical direction in case 1) 70mm sand above riser as shown in fig 4 and graph of Temperature vs Time is plotted as shown in fig.5 Addition of sand above riser top lead to uniform solidification of riser and casting with elongation of solidification time. It is worth to note that in this above case riser and casting solidifying at same rate so solidification curve of all 5 points is overlapping.

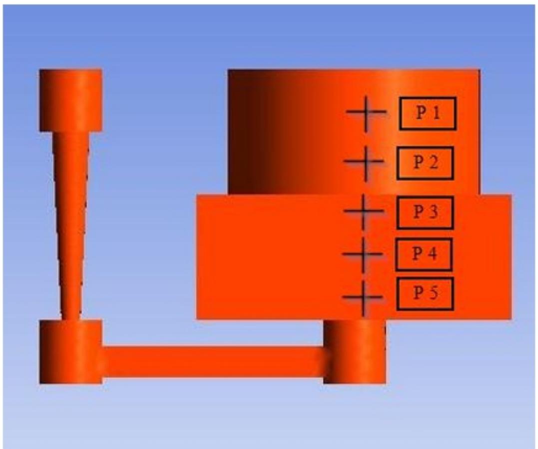

Figure 4. Location of 5 points in casting and riser

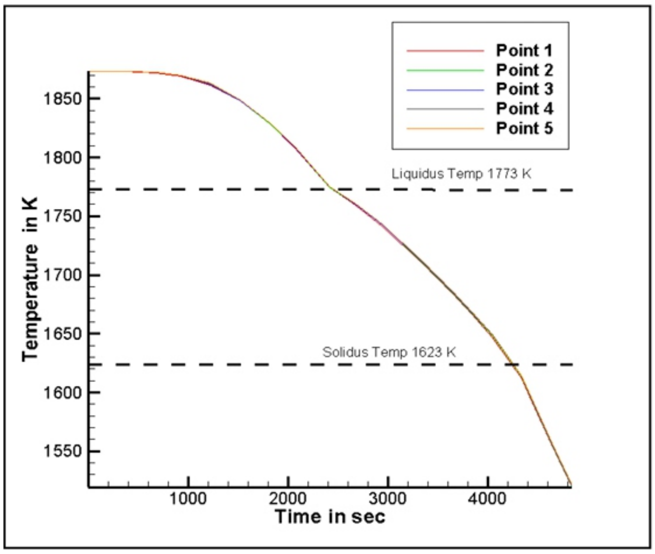

Figure 5. Temp Vs. Time Graph for case 70 mm sand above riser

The direction of solidification is from wall of sand mould to vertical center axis of casting and riser. Similar overlapping solidification curve obtain in other two cases with different solidification time.

while pressure discretization was set to second order. The whole calculation domain state was initialized using standard initialization with phase 2 volume fraction patch to one. Now as casting is filled, multiphase volume of fluid model is turn off. Boundary conditions at sprue inlet and riser outlet are modified to wall condition. Then solver was executed initially with time step 10-05 sec once simulation get stable it increases to 1 sec.

6. RESULT AND DISCUSSION

6.1. Transient thermal behavior of cast solidification without sleeve and hot toppings

Always casting gating system design is carried out in such manner that riser gets solidify at last. But practically when casting is poured it is just possibility that riser gets solidify at last. In casting at different point different cooling rate occurred. Normally highest cooling rate will occurred at near wall and slowest cooling rate is occurred at center or intermediate position. When solidification of casting take place at different point different cooling rate occurred so at different point different temperature exits at that time. The particular region in casting where maximum temperature exist is called as hotspots and this region solidifies at last. To determine solidification time of casting it is necessary to locate hotspot. For that purpose temperature contour at time are plotted as shown in fig. 3

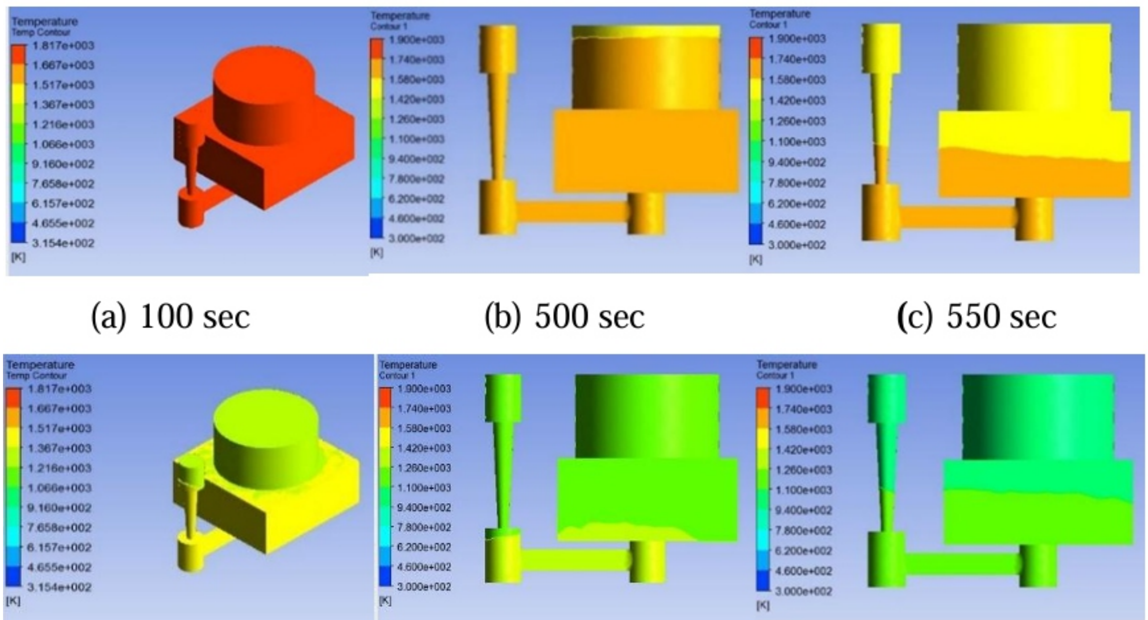

(a) 100 sec (b) 500 sec (c) 550 sec

(d) 1000 sec (e) 1300 sec (f) 1750 sec

Figure 3: Temperature Contour of casting at different instant of time

Time to solidus was found to be 475 sec without exothermic sleeve and hottoping. We can see that directional solidification take place from top of casting to bottom of casting and hotspot occurred at

Result of all three cases is summarize as shown in following table no. 4

Table 4. Result summary of solidification time

Case	Solidification Time
70 mm sand above riser	4800 sec
50 mm sand above riser	4100 sec
20 mm sand above riser	3200 sec

6.2. Transient thermal behavior of cast solidification with sleeve and hot-toppings

The hot toping is another widely used feeding aids. In hot toping thermite material powder is sprayed over riser top surface, similar to exothermic sleeve here also exothermic reaction take place and heat is supplied to riser to elongate its solidification time. Sometimes powder insulating in nature is also mixed with thermite powder to achieve insulation effect at the top riser. In the market the variety of thermal riser sleeve and hottoping are available of unknown material composition in different size and shape. It is heat generation rate of thermite material and burn time on which performance of feeding aids depend instead of geometrical parameter. Here numerical simulation is conducted to investigate the effect of hottoping thickness and heat generation on solidification of riser.

6.2.1. Effect of hottoping thickness

The computational domain involves rectangular casting block with cylindrical riser surrounded by exothermic sleeve of 5mm, at top of riser hot toping of variable thickness is provided and this all domain surrounded by sand mould. In this simulation volumetric heat generation 2637500 w 3 was provided inside exothermic sleeve and hottoping for 40 sec. Following cases are simulated – 1) 6 mm hottoping thickness 2) 4 mm hottoping thickness 3) 2 mm hottoping thickness

To determine solidification time of casting it is necessary to locate hotspot. To determine solidification temperature 5 points are taken along vertical direction in case 1) 6mm hottoping thickness as shown in fig 4 and graph of Temperature vs. Time is plotted as shown in fig.6

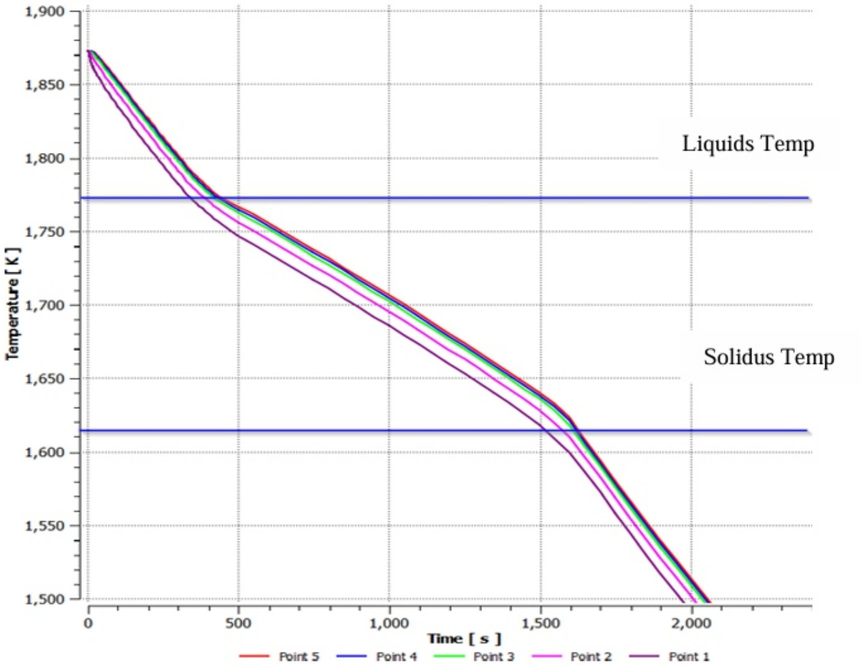

Figure 6. Graph of Temp Vs. Time for Case 1) 6 mm hottoping thickness

Here point P1 and P2 are in riser while P3, P4 and P5 occur in the casting block. From above graph we can see that point P3, P4 and P5 are solidifying before point P1 and P2. So riser is serving it purpose as reservoir. Similar result obtain in other cases. The effect of hottoping thickness on solidification time are summarize as below in table no.5

Table 5: Effect of hottoping thickness on solidification time

Case	Solidification Time
6 mm hot toping thickness	1650 sec
4 mm hot toping thickness	1625 sec
2 mm hot toping thickness	725 sec

Increase in Hottoping thickness lead to elongation in solidification time.

6.2.2. Effect of Variable Heat generation

To evaluate the effect of variable heat generation the computational domain under consideration is rectangular casting block with cylindrical riser surrounded by exothermic sleeve of 5mm, at top of riser 4 mm hot toping is provided and this all domain surrounded by sand mould. Numerical simulation is executed for following cases – 1) Heat Generation rate 1000 KJ/Kg 2) Heat Generation rate 500 KJ/Kg 3) Heat Generation rate 250 KJ/Kg

To determine solidification temperature 5 points are taken along vertical direction in as shown in fig. 4

and graph of Temperature vs. Time is plotted as shown in fig. 7 & 8

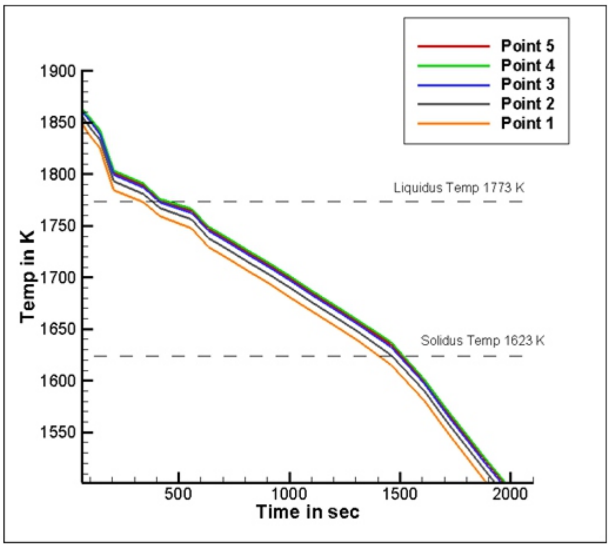

Figure 7. Temp Vs. Time graph case 1) 1000 KJ/Kg

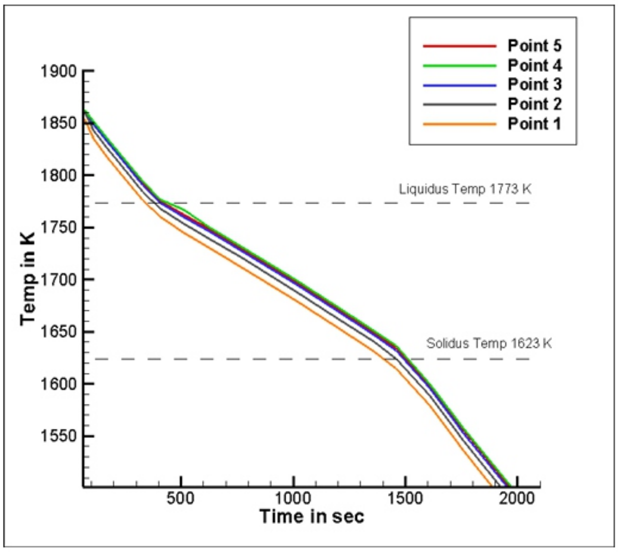

Figure 8. Temp Vs. Time graph case 2) 500 KJ/Kg

Here point P1 and P2 are in riser while P3, P4 and P5 occur in the casting block. From above graph we can see that point P3, P4 and P5 are solidifying before point P1 and P2. So riser is serving it purpose as reservoir. Similar result obtain in other cases. The effect of heat generation on solidification time are summarize as below in table no.6

Table 6 Effect of heat generation on solidification time

Case	Solidification Time
Heat generation rate 1000 KJ/Kg	1525 sec
Heat generation rate 500 KJ/Kg	1550 sec
Heat generation rate 250 KJ/Kg	1650 sec

6. CONCLUSION

Casting with open riser leads to diffusion of heat from riser at much higher rate comparatively to casting block and results in solidification of riser before solidification of casting block.

Addition of sand above riser top leads to elongation of solidification time and simultaneous solidification of casting and riser.

The combination of exothermic sleeve and hottoping leads to formation of favorable temperature gradient. Increase in thickness of hottoping results in elongation of solidification time while increase in heat generation rate leads to decrease in solidification time.

REFERENCES

Wlodawer, R., "The Calculation of Exothermic Feeder Head Materials" Chapter 12 in Directional Solidification of Steel Castings 1st Ed., pp. 163-214,

Pergamon Press, New York, 1966.

Foseco, "Measuring the thermal efficiency of feeding aids", Foundry Practice. 205, 6–10 (1982)

R.A. Hardin, T.J. Williams, C. Beckermann, "Riser sleeve properties for steel castings and the effect of sleeve type on casting yield", in Proceedings of the 67th SFSA Technical and Operating Conference. Paper No. 5.2, Steel Founders' Society of America (SFSA), Chicago, IL (2013).

Midea, A. C., Burns, M., Schneider, M., Wagner, I., "Advanced ThermoPhysical Data for Casting Process Simulation – The Importance of Accurate Riser Sleeve Properties," International Foundry Research, vol. 59, pp. 34-43, 2007.

Zenon Iganszak , Pawel Popielarski "Problems of Heat Source Modeling in Isoexothermic Materials Used as Riser Sleeves in Foundry" 2006.

Thomas J Williams, Richard A Hardin, and Christoph Beckermann "Characterization of the Thermophysical Properties of Riser Sleeve Materials and Analysis of Riser Sleeve Performance", Proceedings of the 69th SFSA, 2015

Thomas J. Williams, Richard A. Hardin & Christoph Beckerman, "Thermophysical Properties and Performance of Riser Sleeves for Steel Castings" International Journal of Metal casting, ISSN 1939-5981 Volume 10 Number.4 (2016)

C. M. Choudhari, B. E. Narkhede, S. K. Mahajan, "Optimum Design and Analysis of Riser for Sand Casting" 2013.

Wiwik Purwadi, Dewi Idamayanti, Cecep Ruskandi, and Jaenudin Kamal, "Effect of shape variation on feeding efficiency for local exothermic-insulating sleeve" Proceedings of the International Mechanical Engineering and Engineering Education Conferences (IMEEEC 2016)

Yuwen X., Chen L., Han Y., "Numerical Simulation of Casting Filling Process Based on FLUENT", International Conference on Future Electrical Power and Energy Systems 2012

ISSN Application No. 21651

Application of Chebyshev Wavelets to Ordinary Differential Equations

Lakshmi B. N.1, Sumana K. P.2, Asha C. S.3, Achala L. N.4
1,2,3,4 P. G. Department of Mathematics and Research Centre in Applied Mathematics, M E S College of Arts, Commerce and Science, Malleswaram, Bengaluru, Karnataka -560003, India.

A B S T R A C T

In this paper, we have solved linear and nonlinear, initial and boundary value problems using Chebyshev wavelet collocation method. In this method, the differential equations are converted to system of linear algebraic equations which can be easily evaluated. Quasilinearization technique is used to handle the nonlinear terms arising in the differential equations. The results obtained are compared with the exact solution. We observe that the Chebyshev wavelet solutions agree with the exact solutions and the same has been depicted through tables and graphs.

Keywords: *Wavelets, Chebyshev wavelets, Differential equations, Quasilinearization, Collocation points.*

1 INTRODUCTION

Wavelet is a trending new method to solve the difficult problems emerging in the field of mathematics, physics and engineering. The concept of 'ondelettes' or 'wavelets' originated from the study of time-frequency signal analysis, wave propagation, and sampling theory [1, 2]. In 1909, the 'wavelets' were first studied in a thesis by Alfred Haar and then the theoretical form was first proposed by Jean Morlet et al. [3] in the Marseille Theoretical Physics Center. Later, in 1988, wavelet analysis has been developed mainly by Y. Meyer and S. Mallat [4].

Wavelets are powerful mathematical tools which are considered abundantly to obtain accurate solutions of integral and differential equations [6]. Wavelets have gained popularity because of their ability to study the functions at different scale features. We come across different wavelet families applied to different studies like for example

Haar, Daubechies, Chebyshev, Legendre and B-Spline wavelets. Chebyshev wavelet is constructed from Chebyshev polynomial as their basis functions. They have excellent interpolating property and gives better accuracy for numerical approximations [5].

Wavelets have many application in signal and image processing like compression, denoising, discontinuity detection, audio enhancement and effects, edge detection, image fusion, image enhancement and many other applications. Recently, the methods based on the orthogonal functions and polynomials series, including wavelets are being used to approximate the solution of various problems. The main advantage of using orthogonal basis is that, it reduces these problems into systems of algebraic equations [5].

Awashie et al. [5] applied the Chebyshev wavelets for simulating a two-phase flow of immiscible fluids in a reservoir with different capillary effect. They observed that the discontinuities exist in the two-phase flow which are caused by the capillary pressure as expected physically. Adibi et al. [6] obtained the numerical solution of Fredholm integral equations of the first kind using Chebyshev wavelets. Hosseini et al. [7] used Chebyshev wavelet collocation method to solve ordinary differential equations. They tested spectral method for the same work which doesn't work well for ordinary differential equations. They also applied the Chebyshev wavelet Galerkin method for these kind of problems.

Celik [8] applied Chebyshev wavelet collocation method to determine the solution of linear ordinary differential equations of second order. They also obtained the approximate solution of Bessel differential equation of order zero and the Lane-Emden equation using the same method. Celik [2] also solved a class of linear and nonlinear nonlocal boundary value problems of second and fourth order using Chebyshev wavelet collocation method. Shiralashetti et al. [9] employed Chebyshev wavelet collocation method to obtain the solution of linear and nonlinear ordinary differential equations. Heydari et al. [10] obtained the solution of partial differential equations using Chebyshev wavelet collocation method.

Oruc et al. [11] considered the one dimensional time dependent coupled Burger's equation along with the suitable initial and boundary conditions. The numerical solutions of this equation is obtained by using Chebyshev wavelet collocation method.Usman et al. [12] considered MHD 3-D fluid flow in the presence of slip and thermal radiation effects and solved using Chebyshev wavelets. They observed that a suitable selection of stretching ratio parameter will help in hastening the heat transfer rate for a fixed value of velocity slip parameter and in reducing the viscous drag over the stretching sheet. Also efficiency of the method was shown by convergent analysis. In order to solve single or systems of nonlinear ordinary and partial differential equations, Bellman and Kalaba [13] introduced the quasilinearization approach as a generalization of the Newton-Raphson method. This technique has quadratic rate of convergence [14, 15]. In this paper, we have considered the Chebyshev wavelet collocation method along with quasilinearization technique to obtain the numerical solution of linear and nonlinear, initial and boundary value problems.

2 CHEBYSHEV WAVELETS

Wavelets constitute a family of functions constructed from dilation and translation of a single functions called as the Mother wavelet. If this dilation parameter and translation parameter are allowed to vary continuously then, we get a family of continuous wavelets [11],

$$\psi_{a,b}(x) = |a|^{-\frac{1}{2}} \psi\left(\frac{x-b}{a}\right),$$

where $a, b \in \mathbb{R}, a \neq 0$.

The family of Chebyshev wavelets [2] are defined in the interval $[0, 1)$ as,

$$C_i(x) = C_{nm}(x) = \begin{cases} \dfrac{\alpha_m 2^{\frac{k}{2}}}{\sqrt{\pi}} T_m(2^k x - 2n + 1), & \dfrac{n-1}{2^{k-1}} \leq x \leq \dfrac{n}{2^{k-1}} \\ 0\,, & \text{otherwise} \end{cases} \dots\dots\dots\dots (1)$$

where

$$\alpha_m = \begin{cases} \sqrt{2}, & m = 0 \\ 2, & \text{otherwise} \end{cases}$$

where $i = n + 2^{k-1}m, k$ is any positive integer, $n = 1,2, \dots, 2^{k-1}, m = 0,1,2, \dots, M - 1, M$ is the maximum degree of Chebyshev wavelets of first kind and x is the normalized time. $T_m(x)$ are Chebyshev polynomials of degree m which are orthogonal with respect to the weight function $\omega(x) = \frac{1}{\sqrt{1-x^2}}$ on $[-1, 1]$. The Chebyshev polynomials satisfy the following recurrence formula,

$$T_0(x) = 1, T_1(x) = x, T_{m+1} = 2xT_m(x) - T_{m-1}(x), \qquad \forall\, m = 1,2,3, \dots.$$

The wavelet collocation points are defined as

$$x_j = \frac{j - 0.5}{N}, \qquad \forall\ j = 1,2, \dots, N,$$

where $N = 2^{k-1}M$.

In order to solve the differential equations of second order, we require the following integrals.

$$P_i(x) = \int_0^x C_i(x)dx \ \ and \ \ Q_i(x) = \int_0^x P_i(x)dx\,.$$

2.1 FUNCTION APPROXIMATION

A function $f(x)$ which is square integrable on $[0,1)$ can be expressed as infinite sum of Chebyshev wavelets as [5],

$$f(x) = \sum_{n=1}^{\infty} \sum_{m=0}^{\infty} a_{nm} C_{nm}(x) \dots\dots\dots\dots (2)$$

where

$$a_{nm} = \int_0^1 f(x) C_{nm}(x) \omega_n(x) dx \ldots\ldots\ldots\ldots (3)$$

If the function $f(x)$ is approximated as piecewise constant in each subinterval, then equation (2) becomes

$$f(x) = \sum_{n=1}^{2^{k-1}} \sum_{m=0}^{M-1} a_{nm} C_{nm}(x) \ldots\ldots\ldots\ldots (4)$$

where a_{nm} are the Chebyshev wavelet coefficients to be determined.

3 METHOD OF SOLUTION

In this section, the Chebyshev wavelet collocation method (CWCM) is used to solve the linear and nonlinear, initial and boundary value problems.

Example 1:

Consider the linear ordinary differential equation of the form,

$$y'' - 3y' + 2y = 6e^{-x} \ldots\ldots\ldots\ldots (5)$$

with initial conditions

$$y(0) = 2\,, y'(0) = 2 \ldots\ldots\ldots\ldots (6)$$

and the exact solution is $y(x) = 2e^{2x} - e^{x} - e^{-x}$.

The Chebyshev wavelet solution of the form,

$$y''(x) = \sum_{i=1}^{N} a_i\, C_i(x) \;\; \ldots\ldots\ldots\ldots\; (7)$$

where $a_i's,\; i = 1,2, \ldots, N$ are Chebyshev wavelet coefficients to be determined.

Integrating equation (7) twice with respect to x from 0 to x and using equation (6), we get

$$y'(x) = 2 + \sum_{i=1}^{N} a_i\, P_i(x) \ldots\ldots\ldots\ldots (8)$$

$$y(x) = 2 + 2x + \sum_{i=1}^{N} a_i\, Q_i(x) \ldots\ldots\ldots\ldots (9)$$

Substituting equations (7), (8) and (9) in (5), we obtain

$$\sum_{i=1}^{N} a_i \left(C_i(x) - 3P_i(x) + 2Q_i(x)\right) = 6e^{-x} - 4x + 2 \;\ldots\ldots\ldots\ldots\; (10)$$

Taking the collocation points $x = x_j$ in equations (10) and (9), we have

$$\sum_{i=1}^{N} a_i \left(C_i(x_j) - 3P_i(x_j) + 2Q_i(x_j)\right) = 6e^{-x_j} - 4x_j + 2 \ldots\ldots\ldots\ldots\; (11)$$

$$y(x_j) = 2 + 2x_j + \sum_{i=1}^{N} a_i\, Q_i(x_j) \ldots\ldots\ldots\ldots\; (12)$$

The wavelet coefficients $a_i,\ i = 1,2,\ldots,N$ are obtained by solving the N system of equations obtained in equation (11). These coefficients are then substituted in equation (12) to obtain the Chebyshev wavelet solutions at the collocation points $x_j, j = 1,2,\ldots,N$. Table 1 shows the comparison of CWCM and exact solution. Figure 1 depicts the typical behaviour of the solution for $k = 3, M = 10$.

EXAMPLE 2:

Consider the nonlinear ordinary differential equation with initial conditions

$$y'' + y' + y + y^2\, y' = -sin\, x - sin\, x \cos^2 x \ldots\ldots\ldots\ldots\; (13)$$

$$y(0) = 1\,, y'(0) = 0 \ldots\ldots\ldots\ldots\; (14)$$

The exact solution is $y(x) = cos\ x$.

As illustrated in example 1, we have

$$y''(x) = \sum_{i=1}^{N} a_i\, C_i(x) \;\ldots\ldots\ldots\ldots\; (15)$$

$$y' = \sum_{i=1}^{N} a_i\, P_i(x) \;\ldots\ldots\ldots\ldots\; (16)$$

$$y(x) = 1 + \sum_{i=1}^{N} a_i\, Q_i(x) \;\ldots\ldots\ldots\ldots\; (17)$$

where $a_i's,, i = 1,2,\ldots,N$ are Chebyshev wavelet coefficients to be determined. Using quasilinearization technique to handle the nonlinear terms in equation (13), we get

$$y''_{r+1} + (1 + y_r^2)y'_{r+1} + (1 + 2y_r y'_r)y_{r+1} = 2y_r^2\, y'_r - \sin x - \sin x\, cos^2 x$$

$$\ldots\ldots\ldots\ldots\; (18)$$

Substituting equations (15), (16) and (17) in equation (18) and taking the collocation points $x = x_j$, we obtain

$$\sum_{i=1}^{N} a_i \left(C_i(x_j) + (1 + y_r^2) P_i(x_j) + (1 + 2 y_r y_r') Q_i(x_j) \right) =$$
$$2 y_r^2 \, y_r' - \sin x_j - \sin x_j \, cos^2 x_j - (1 + 2 y_r y_r') \dots \dots \dots \dots \; (19)$$

$$y(x_j) = 1 + \sum_{i=1}^{N} a_i \, Q_i(x_j) \dots \dots \dots \dots \; (20)$$

Further, equation (19) is solved to get the wavelet coefficients $a_i, i = 1,2, \dots, N$ which are used to obtain the Chebyshev wavelet solutions at the collocation points $x_j, j = 1,2, \dots, N$ from equation (20). For $k = 3, M = 10$ Table 2 represents the comparison of CWCM and the exact solution. The approximate solution and the exact solution are plotted in

Figure **2**.

EXAMPLE 3:

Consider the linear ordinary differential equation with boundary conditions

$$y'' + y = 1 \dots \dots \dots \dots \; (21)$$

$$y(0) = 0 \, , y(1) = 1 \dots \dots \dots \dots \; (22)$$

and the exact solution is given by $y(x) = -cos \, x + cot1 \, sin \, x + 1$.

The Chebyshev wavelet solution is of the form,

$$y''(x) = \sum_{i=1}^{N} a_i \, C_i(x) \dots \dots \dots \dots \; (23)$$

where $a_i's, \; i = 1,2, \dots, N$ are Chebyshev wavelet coefficients to be determined.

Integrating equation (23) twice with respect to x from 0 to x and using equation (22), we get

$$y'(x) = y'(0) + \sum_{i=1}^{N} a_i \, P_i(x) \dots \dots \dots \dots \; (24)$$

$$y(x) = x y'(0) + \sum_{i=1}^{N} a_i \, Q_i(x) \dots \dots \dots \dots \; (25)$$

Putting $x = 1$ in equation (25) and using equation (22), we obtain

$$y'(0) = 1 - \sum_{i=1}^{N} a_i \, Q_i(1) \dots \dots \dots \dots \; (26)$$

Substituting equation (26) in equations (24) and (25), we get

$$y'(x) = 1 + \sum_{i=1}^{N} a_i \left(P_i(x) - Q_i(1)\right) \dots\dots\dots\dots (27)$$

$$y(x) = x + \sum_{i=1}^{N} a_i \left(Q_i(x) - xQ_i(1)\right) \dots\dots\dots\dots (28)$$

Substituting equations (23) and (28) in (21), leads to

$$\sum_{i=1}^{N} a_i(C_i(x) + Q_i(x) - xQ_i(1)) = 1 - x \dots\dots\dots\dots (29)$$

Taking the collocation points $x = x_j$ in equations (29) and (28), we have

$$\sum_{i=1}^{N} a_i \left(C_i(x_j) + Q_i(x_j) - x_jQ_i(1)\right) = 1 - x_j \dots\dots\dots\dots (30)$$

$$y(x_j) = x_j + \sum_{i=1}^{N} a_i \left(Q_i(x_j) - x_jQ_i(1)\right) \dots\dots\dots\dots (31)$$

The N system of equations in equation (30) are solved in order to determine the wavelet coefficients $a_i, i = 1,2,\dots,N$. Then the Chebyshev wavelet solutions at the collocation points $x_j, j = 1,2,\dots,N$ are obtained by using the wavelet coefficients values in (31). In

Figure **3** we plot the numerical solution and exact solution and values are tabulated in Table 3 for $k = 3, M = 10$.

EXAMPLE 4:

Consider the nonlinear ordinary differential equation with boundary conditions

$$y'' - yy' = -\frac{1}{4\sqrt{(1+x)^3}} - \frac{1}{2} \dots\dots\dots\dots (32)$$

$$y(0) = 1\,, y(1) = \sqrt{2} \dots\dots\dots\dots (33)$$

The exact solution is $y(x) = \sqrt{1+x}$.
As illustrated in example 3, we have

$$y''(x) = \sum_{i=1}^{N} a_i\, C_i(x) \dots\dots\dots\dots (34)$$

$$y'(x) = \sqrt{2} - 1 + \sum_{i=1}^{N} a_i \left(P_i(x) - Q_i(1)\right) \dots\dots\dots\dots (35)$$

$$y(x) = 1 + (\sqrt{2} - 1)x + \sum_{i=1}^{N} a_i \left(Q_i(x) - xQ_i(1)\right) \dots\dots\dots\dots (36)$$

where $a_i's, i = 1,2,\dots,N$ are Chebyshev wavelet coefficients to be determined. The nonlinear terms in equation (32) are handled using quasilinearization technique, which leads to

$$y''_{r+1} - y'_{r+1}\, y_r - y_{r+1} y'_r = -y_r\, y'_r - \frac{1}{4\sqrt{(1+x)^3}} - \frac{1}{2} \dots\dots\dots\dots (37)$$

Substituting equations (34) and (36) in equation (37) and taking the collocation points $x = x_j$, we obtain

$$\sum_{i=1}^{N} a_i\big(C_i(x_j) - y_r(P_i(x_j) - Q_i(1)) - y'_r(Q_i(x_j) - x_j Q_i(1))\big) = \big(\sqrt{2}-1\big)y_r$$

$$+\big(1 + \big(\sqrt{2}-1\big)x_j\big)y'_r - y_r\, y'_r - \frac{1}{4\sqrt{\big(1+x_j\big)^3}} - \frac{1}{2} \dots\dots\dots\dots (38)$$

$$y(x_j) = 1 + \big(\sqrt{2}-1\big)x_j + \sum_{i=1}^{N} a_i\,\big(Q_i(x_j) - x_j Q_i(1)\big) \dots\dots\dots\dots (39)$$

Using equation (38), we obtain the wavelet coefficients $a_i, i = 1,2,\dots,N$ which are substituted in equation (39) to determine the Chebyshev wavelet solutions at the collocation points $x_j, j = 1,2,\dots,N$. In Table 4 we compare the results obtained by CWCM with the exact solutions for $k = 3, M = 10$ and the behaviour of the solution is shown in

Figure **4**.

4 CONCLUSION

In this paper, the Chebyshev wavelet collocation method is applied to linear and nonlinear, initial and boundary value problems. The method converts differential equation to system of algebraic equations which can be solved easily. The results obtained are in good agreement with the exact solution. The accuracy of the results are high even for small number of grid points. We analyse from the tables and graphs that the CWCM solutions are very close to the exact solutions. In the case of boundary value problems this method is very convenient as it takes care of the boundary conditions automatically. Thus the method is simple, reliable and highly efficient.

Table 1: Comparison of CWCM and exact solution of example 1.

x	y(x)	
	CWCM	Exact
0.125000	2.317301	2.317399
1.125000	16.215125	16.219907
2.125000	131.911217	131.957360
3.125000	1012.759350	1013.309691
4.125000	7588.276111	7593.399997
5.125000	56354.014350	56396.915645
6.125000	417090.821054	417505.435214
7.125000	3083782.397952	3087106.286808
8.125000	22787375.548094	22816605.660021
9.125000	168369534.307553	168608956.465621

Table 2: Comparison of CWCM and exact solution of example 2.

x	y(x)	
	CWCM	Exact
0.125000	0.9921976670	0.9921976672
1.125000	0.4311765159	0.4311765168
2.125000	-0.5262663355	-0.5262663347
3.125000	-0.9998623443	-0.9998623451
4.125000	-0.5541895254	-0.5541895265
5.125000	0.4010025879	0.4010025870
6.125000	0.9875147715	0.9875147713
7.125000	0.6661104290	0.6661104290
8.125000	-0.2677127712	-0.2677127697
9.125000	-0.9554020839	-0.9554020827

Table 3: Comparison of CWCM and exact solution of example 3.

x	y(x)	
	CWCM	Exact
0.012500	0.00810407266904134	0.00810407266904123

0.112500	0.07840459771933983	0.07840459771933983
0.212500	0.15791339939028937	0.15791339939028937
0.312500	0.24583605201770939	0.24583605201770942
0.412500	0.34129406151991160	0.34129406151991160
0.512500	0.44333364302017275	0.44333364302017264
0.612500	0.55093525074994343	0.55093525074994343
0.712500	0.66302376501315008	0.66302376501315008
0.812500	0.77847923442681177	0.77847923442681177
0.912500	0.89614806610505104	0.89614806610505093

Table 4: Comparison of CWCM and exact solution of example 4.

x	**y(x)**	
	CWCM	**Exact**
0.012500	1.006230589874905	1.006230589874905
0.112500	1.054751155486445	1.054751155486449
0.212500	1.101135777277254	1.101135777277262
0.312500	1.145643923738950	1.145643923738960
0.412500	1.188486432400462	1.188486432400471
0.512500	1.229837387624876	1.229837387624884
0.612500	1.269842509920022	1.269842509920029
0.712500	1.308625232830234	1.308625232830240
0.812500	1.346291201783623	1.346291201783626
0.912500	1.382931668593931	1.382931668593933

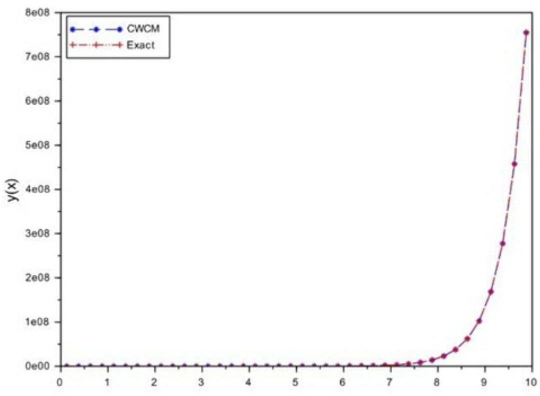

Figure 1: Comparison of CWCM and exact solution of example 1.

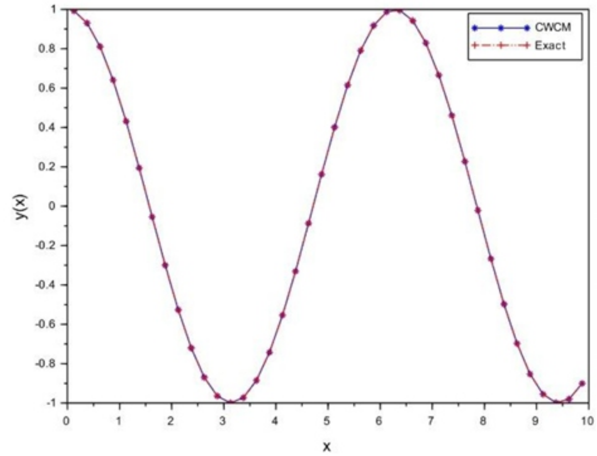

Figure 2: Comparison of CWCM and exact solution of example 2.

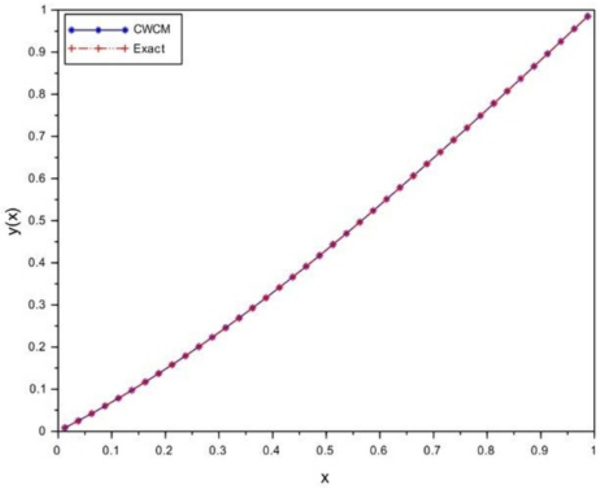

Figure 3: Comparison of CWCM and exact solution of example 3.

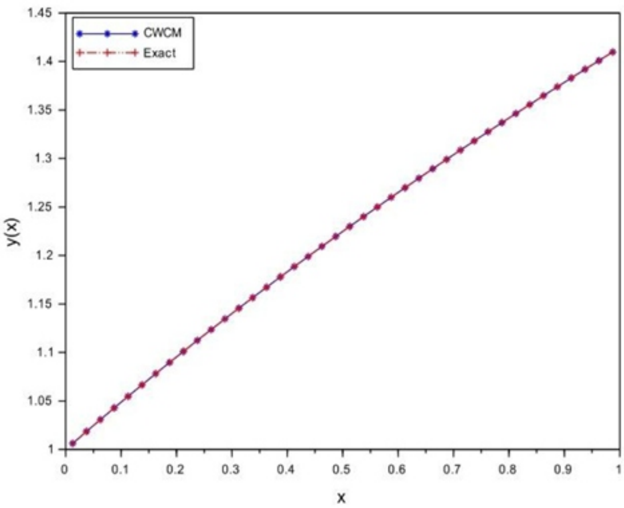

Figure 4: Comparison of CWCM and exact solution of example 4.

REFERENCES

1. Debnath, L., & Shah, F. A. (2002). Wavelet transforms and their applications (pp. 12-14). Boston: Birkhäuser.

2. Çelik, İ. (2018). Chebyshev Wavelet collocation method for solving a class of linear and nonlinear nonlocal boundary value problems. Fundamental Journal of Mathematics and Applications, 1(1), 25-35.

3. Rajini, G. K. (2016). A comprehensive review on wavelet transform and its applications. ARPN Journal of Engineering and Applied Sciences, 11(19), 11713.

4. Chun-Lin, L. (2010). A tutorial of the wavelet transform. NTUEE, Taiwan, 21,22.

5. Awashie, G. E., Amoako-Yirenkyi, P., & Dontwi, I. K. (2019). Chebyshev wavelets collocation method for simulating a two-phase flow of immiscible fluids in a reservoir with different capillary effects. Journal of Petroleum Exploration and Production Technology, 9(3), 2039-2051.

6. Adibi, H., & Assari, P. (2010). Chebyshev wavelet method for numerical solution of Fredholm integral equations of the first kind. Mathematical problems in Engineering, 2010.

7. Hosseini, S. G., & Mohammadi, F. (2011). A new operational matrix of derivative for Chebyshev wavelets and its applications in solving ordinary differential equations with non-analytic solution. Applied mathematical sciences, 5(51), 2537-2548.

8. Celik, I. (2013). Numerical solution of differential equations by using Chebyshev wavelet collocation method. Cankaya university journal of science and engineering, 10(2).

9. Shiralashetti, S. C., & Deshi, A. B. (2017). Chebyshev Wavelet Collocation Method for the Numerical Solution of Ordinary Differential Equations. Journal of the Nigerian Mathematical Society, 36(2), 337-353.

10. Heydari, M. H., Hooshmandasl, M. R., & Ghaini, F. M. (2014). A new approach of the Chebyshev wavelets method for partial differential equations with boundary conditions of the telegraph type. Applied Mathematical Modelling, 38(5-6), 1597-1606.

11. Oruç, Ö. Bulut, F., & Esen, A. L. A. A. T. T. İ. N. (2019). Chebyshev wavelet method for numerical solutions of coupled Burgers' equation. Hacettepe Journal of Mathematics and Statistics, 48(1), 1-16.

12. Usman, M., Zubair, T., Hamid, M., Haq, R. U., & Wang, W. (2018). Waveles solution of MHD 3-D fluid flow in the presence of slip and thermal radiation effects. Physics of Fluids, 30(2), 023104.

13. Bellman, R. E., & Quasilinearization, R. K. (1965). Nonlinear Boundary-Value Problems. American Elsevier Publishing Co., Inc., New York.

14. Saeed, U. (2014, January). Wavelet-Galerkin quasilinearization method for nonlinear boundary value problems. In Abstract and Applied Analysis (Vol. 2014). Hindawi.

15. Iqbal, M. A., Khan, U., Ali, A., & Mohyud-Din, S. T. (2015). Shifted Chebyshev wavelet-

quasilinearization technique for MHD squeezing flow between two infinite plates and Jeffery–Hamel flows. Egyptian Journal of Basic and Applied Sciences, 2(3), 229-235.

Instructions for Authors

Essentials for Publishing in this Journal

1 Submitted articles should not have been previously published or be currently under consideration for publication elsewhere.

2 Conference papers may only be submitted if the paper has been completely re-written (taken to mean more than 50%) and the author has cleared any necessary permission with the copyright owner if it has been previously copyrighted.

3 All our articles are refereed through a double-blind process.

4 All authors must declare they have read and agreed to the content of the submitted article and must sign a declaration correspond to the originality of the article.

Submission Process

All articles for this journal must be submitted using our online submissions system. http://enrichedpub.com/ . Please use the Submit Your Article link in the Author Service area.

Manuscript Guidelines

The instructions to authors about the article preparation for publication in the Manuscripts are submitted online, through the e-Ur (Electronic editing) system, developed by **Enriched Publications Pvt. Ltd**. The article should contain the abstract with keywords, introduction, body, conclusion, references and the summary in English language (without heading and subheading enumeration). The article length should not exceed 16 pages of A4 paper format.

Title

The title should be informative. It is in both Journal's and author's best interest to use terms suitable. For indexing and word search. If there are no such terms in the title, the author is strongly advised to add a subtitle. The title should be given in English as well. The titles precede the abstract and the summary in an appropriate language.

Letterhead Title

The letterhead title is given at a top of each page for easier identification of article copies in an Electronic form in particular. It contains the author's surname and first name initial .article title, journal title and collation (year, volume, and issue, first and last page). The journal and article titles can be given in a shortened form.

Author's Name

Full name(s) of author(s) should be used. It is advisable to give the middle initial. Names are given in their original form.

Contact Details

The postal address or the e-mail address of the author (usually of the first one if there are more Authors) is given in the footnote at the bottom of the first page.

Type of Articles

Classification of articles is a duty of the editorial staff and is of special importance. Referees and the members of the editorial staff, or section editors, can propose a category, but the editor-in-chief has the sole responsibility for their classification. Journal articles are classified as follows:

Scientific articles:

1. Original scientific paper (giving the previously unpublished results of the author's own research based on management methods).
2. Survey paper (giving an original, detailed and critical view of a research problem or an area to which the author has made a contribution visible through his self-citation);
3. Short or preliminary communication (original management paper of full format but of a smaller extent or of a preliminary character);
4. Scientific critique or forum (discussion on a particular scientific topic, based exclusively on management argumentation) and commentaries. Exceptionally, in particular areas, a scientific paper in the Journal can be in a form of a monograph or a critical edition of scientific data (historical, archival, lexicographic, bibliographic, data survey, etc.) which were unknown or hardly accessible for scientific research.

Professional articles:

1. Professional paper (contribution offering experience useful for improvement of professional practice but not necessarily based on scientific methods);
2. Informative contribution (editorial, commentary, etc.);
3. Review (of a book, software, case study, scientific event, etc.)

Language

The article should be in English. The grammar and style of the article should be of good quality. The systematized text should be without abbreviations (except standard ones). All measurements must be in SI units. The sequence of formulae is denoted in Arabic numerals in parentheses on the right-hand side.

Abstract and Summary

An abstract is a concise informative presentation of the article content for fast and accurate Evaluation of its relevance. It is both in the Editorial Office's and the author's best interest for an abstract to contain terms often used for indexing and article search. The abstract describes the purpose of the study and the methods, outlines the findings and state the conclusions. A 100- to 250-Word abstract should be placed between the title and the keywords with the body text to follow. Besides an abstract are advised to have a summary in English, at the end of the article, after the Reference list. The summary should be structured and long up to 1/10 of the article length (it is more extensive than the abstract).

Keywords

Keywords are terms or phrases showing adequately the article content for indexing and search purposes. They should be allocated heaving in mind widely accepted international sources (index, dictionary or thesaurus), such as the Web of Science keyword list for science in general. The higher their usage frequency is the better. Up to 10 keywords immediately follow the abstract and the summary, in respective languages.

Acknowledgements

The name and the number of the project or programmed within which the article was realized is given in a separate note at the bottom of the first page together with the name of the institution which financially supported the project or programmed.

Tables and Illustrations

All the captions should be in the original language as well as in English, together with the texts in illustrations if possible. Tables are typed in the same style as the text and are denoted by numerals at the top. Photographs and drawings, placed appropriately in the text, should be clear, precise and suitable for reproduction. Drawings should be created in Word or Corel.

Citation in the Text

Citation in the text must be uniform. When citing references in the text, use the reference number set in square brackets from the Reference list at the end of the article.

Footnotes

Footnotes are given at the bottom of the page with the text they refer to. They can contain less relevant details, additional explanations or used sources (e.g. scientific material, manuals). They cannot replace the cited literature.
The article should be accompanied with a cover letter with the information about the author(s): surname, middle initial, first name, and citizen personal number, rank, title, e-mail address, and affiliation address, home address including municipality, phone number in the office and at home (or a mobile phone number). The cover letter should state the type of the article and tell which illustrations are original and which are not.